# Crystallization of Eflucimibe Drug in a Solvent Mixture: Effects of Process Conditions on Polymorphism

**ARTICLE** *in* CRYSTAL GROWTH & DESIGN · FEBRUARY 2004

Impact Factor: 4.89 · DOI: 10.1021/cg0341961



**3 AUTHORS**, INCLUDING:

Sébastien Teychené
Laboratory of Chemical Engineering - LGC
**24** PUBLICATIONS **139** CITATIONS
SEE PROFILE

Béatrice Biscans
French National Centre for Scientific Research
**91** PUBLICATIONS **706** CITATIONS
SEE PROFILE

CRYSTAL GROWTH & DESIGN
2004
VOL. 4, NO. 5
971−977

# Crystallization of Eflucimibe Drug in a Solvent Mixture: Effects of Process Conditions on Polymorphism

Sébastien Teychené,*,† Jean M. Autret,‡ and Béatrice Biscans†

*Laboratoire de Génie Chimique, UMR 5503, CNRS/INPT/UPS, 5 Rue Paulin Talabot, BP 1301, 31106 Toulouse Cedex, France, and Laboratoire Pierre Fabre (Plantes et industrie), 16 rue Jean Rostand 81600 Gaillac, France*

*Received October 28, 2003; Revised Manuscript Received January 9, 2004*

**ABSTRACT:** Nucleation and metastability of the eflucimibe (*S*)-2′,3′,5′-trimethyl-4′-hydroxy-dodecylthiophenyl-acetanilide, a new acyl-coenzyme A:cholesterol *O*-acyltransferase (ACAT) inhibitor, have been investigated according to a polythermal method. Eflucimibe exhibits two polymorphs, A and B, which crystallize simultaneously (concomitant polymorphs). The focus of this study was on the effect of the cooling rate, the initial concentration, and the seeds on metastability and polymorphism of eflucimibe. For nonseeded crystallization, it was found that the metastable zone width is large (primary nucleation) and fulfills well the linear relation between log $\Delta T_{max}$ and log($dT/dt$). In addition, the X-ray powder diffraction and differential scanning calorimetry analyses of the powder obtained show that the desired polymorph (pure A form) is difficult to obtain. On the contrary, for seeded experiments, the metastable zone width is significantly reduced (secondary nucleation) and the occurrence of polymorphism is controlled by seeding with the desired polymorph.

## Introduction

Understanding and controlling polymorphism, the ability of a molecule to crystallize in different lattices, remains a subject of broad interest and active research. Conformational polymorphism arises when multiple molecular conformations can be stabilized in the solid state.[1] In that case, crystallization gives rise to polymorphs that differ not only in the mode of packing but also in molecular conformation, and the crystallization tendency may be significantly reduced. The reduction of the crystallization tendency for flexible molecules arises from the presence of multiple conformers in the crystallizing media and the need for certain molecules to crystallize in a high-energy conformation.[2] Moreover, when two conformers A and B are very close energetically and structurally, the nucleation rates are of the same order of magnitude ($J_A - J_B$), and both structures are formed simultaneously (concomitant polymorphs).[3,4]

Recently, the polymorphism of the eflucimibe (*S*)-2′,3′,5′-trimethyl-4′-hydroxy-dodecylthiophenyl-acetanilide, a new acyl-coenzyme A:cholesterol *O*-acyltransferase (ACAT) inhibitor developed by Pierre Fabre research center, has been studied by Ribet and al.[5] In this previous work, different solvents were used to produce crystals (methanol, ethanol, propanol, 2-propanol, ethyl acetate, acetone, methylene chloride, chloroform, acetonitrile, hexane). It was found that eflucimibe crystallizes in two polymorphs identified as A and B, which could differ by a conformational change of the phenol group in the crystal lattice. The characterization of the crystals was based on several types of analytical methods, and the details of these techniques and their interpretation can be found in this previous work.

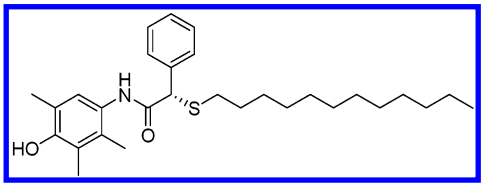


**Figure 1.** Molecular structure of eflucimibe.

The aim of this paper is to study the influence of the crystallization process parameters on the nucleation kinetics of the polymorphs of eflucimibe. The operating parameters studied are the cooling rate, the initial concentration of the solution, and the use of seeds during crystallization. To identify the two forms A and B, our crystallized samples were analyzed by X-ray powder diffraction (XRPD) and differential scanning calorimetry (DSC). The results obtained will be summarized in the first part of this paper.

**Characterization of Eflucimibe. Product.** Eflucimibe ($M$ = 469.73 g mol$^{-1}$, see Figure 1) was supplied by Pierre Fabre, Plantes et Industries. It is a microcrystalline fatty powder with a minimum chemical purity of 99% and was used without further purification.

Two samples of crystals, respectively called A and B, were also supplied. They were prepared by recrystallization of the melt (B form) on one hand and from solution (A form) on the other hand.

**XRPD Studies.** Powders of eflucimibe were studied by XRPD at the European Synchrotron radiation facility in Grenoble, France. The samples were mounted in 1.0-mm borosilicate capillaries and a wavelength of 0.515519(7) Å was selected using a double Si(111) monochromator. Data were collected between 0.75 and 20° 2$\theta$ with an angular resolution of 0.02° 2$\theta$. Samples were heated in air in 0.3 °C steps from 25 to 135 °C. After each 1 °C step, the samples were allowed to equilibrate for 30 s, followed by a 5 s acquisition.

Representative high resolution powder patterns of two pure phases A and B are shown in Figure 2. Both

* To whom correspondence should be addressed. E-mail: Sebastien.Teychene@ensiacet.fr; fax: (+33)5.34.61.52.53; tel: (+33)5.34.61.52.85.
† Laboratoire de Génie Chimique, UMR 5503, CNRS/INPT/UPS.
‡ Laboratoire Pierre Fabre (Plantes et industrie).

10.1021/cg0341961 CCC: $27.50 
Published on Web 02/26/2004

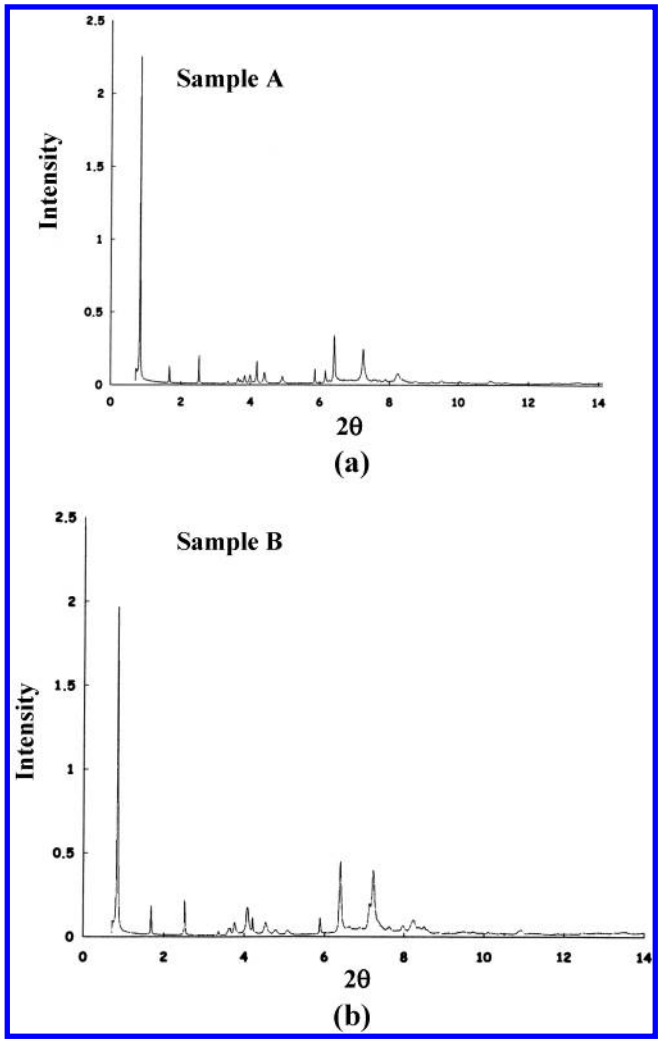


**Figure 2.** High-resolution X-ray powder diffraction patterns of pure phases A (a) and B (b).

samples are rather weakly diffracting, display significant peak broadening, and do not scatter to a very high angle.

Due to the poor crystallinity of the samples, it was not possible to derive even the unit cells from any of the diffraction patterns. Nevertheless, some structural characteristics may be postulated. The first three diffraction peaks (called 00L's) appear to be multiples of a long axis (around 35 Å at room temperature). This is supported by the equivalent thermal expansion behavior of these peaks upon heating. In addition, these peaks and further multiples are sharper than the other peaks, indicating that all belong to the same zone axis. The narrow width of these peaks indicates better crystalline order in this direction. The broadening observed in the non-00L peaks indicates a greater degree of disorder about the long axis, consistent with the prolate form of the molecule. Such a disorder is also presumably the cause of the rapid weakening of scattering with angle. As the first non-00L peaks appear at smaller *d* spacing (<8.2 Å), the other axes seem to be much shorter. Thus, structures for both phases A and B can be assumed, in which the molecules are aligned along the long cell axes. Different phases would then be due to different orientational settings of the molecules about this axis.

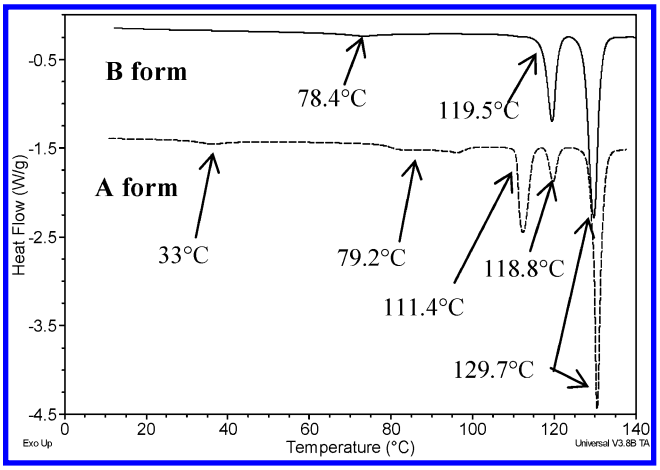


**Figure 3.** Thermal profiles obtained by differential scanning calorimetry of samples A and B.

The heating runs are not reported here, but the results show that all of the features observed seem to be associated with structural phase transitions within two distinct series stemming from polymorphs A and B. That is to say that there is no evidence that a distinct transition occurs between the two polymorphs on heating. This is true for the strong first-order transition observed in the B phase near 75 and 110 °C and for its melting at 130 °C. For the A phase, the first-order transition near 105 °C is clearly present, and two more subtle second- or weakly first-order transitions near 80 and 90 °C can be attested. There is some evidence for further such transition near 35 and 115 °C. Furthermore, the behavior on heating seems to be perfectly reproducible. From these observations, one would be tempted to speculate that there is a conformational difference between the A and B polymorphs.

**Thermal Analysis.** Thermogravimetry analyses of the samples did not show any loss of mass in a temperature range between 25 and 150 °C. The melt decomposition was observed near 200 °C under nitrogen environment.

The DSC scans were recorded on a TA instrument-DSC 2920 modulated at 5 °C/min under nitrogen purge. The temperature and heat flow were calibrated using indium. The sample for DSC analysis was accurately weighed into an aluminum pan and hermetically sealed. The sample was first heated to 140 °C and then cooled to −40 °C.

The DSC curves of the A and B forms (Figure 3) show, respectively, five and three endotherms between 30 and 140 °C. By performing cooling−heating cycles, before melting, the total reversibility of the thermal event was observed. A quench cooling of the melt always led to the formation of the B modification, and according to the Ostwald rule stage, it could be the metastable form compared to phase A. But, as the melting point of each polymorph cannot be determined separately, no conclusion can be drawn for the relative stability in terms of monotropy or enantiotropy.

The DSC results are consistent with all the features observed by XRPD, and no transition between the two forms was observed upon heating.

In conclusion, from these analytical methods and from other techniques previously performed,[5] even in the case of an eventual successful indexing of one of the phases,

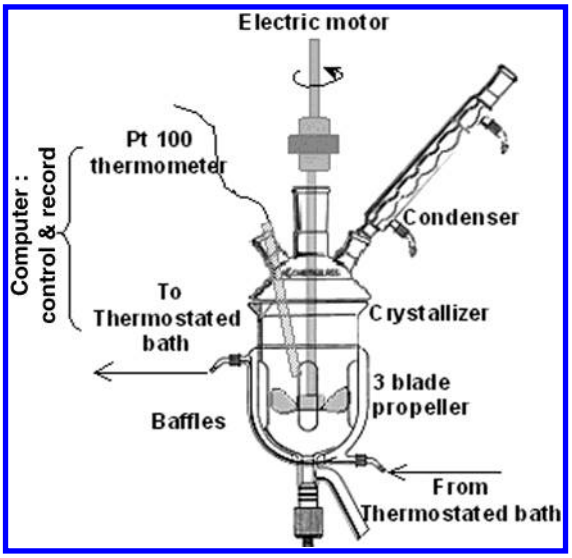


**Figure 4.** Round-bottomed 150-mL crystallizer used for eflucimibe crystallization.

the high degree of disorder present (as indicated by the peak broadening and poor diffracting power at high temperature) makes it highly unlikely that a successful structure determination could be carried out with the powder diffraction data. A single crystal would be necessary. Despite not knowing the crystal structures of the compounds, something about the behavior of their polymorphism nevertheless may be deduced. In the following section, we will refer to the XRPD and DSC patterns shown in Figures 2 and 3, to identify the so-called phases A or B. The product obtained from the crystallization process will be analyzed in the same way and compared to these "pure" A and B forms to obtain a relative proportion of these phases.

## Experimental Section

**Solubility Measurements.** Reagent grade ethanol and *n*-heptane (99.95% purity) were used as pure and mixture solvents and purchased from Prolabo (SA). Crystals of eflucimibe characterized by XRPD and DSC and identified, respectively, as the A form and B form, were used for the solubilities determination. Experiments were carried out, in the binary systems (eflucimibe/ethanol and eflucimibe/*n*-heptane) and in the ternary system (eflucimibe/ethanol/*n*-heptane). The drug solubility was determined according to a usual procedure: sealed flasks containing an excess of powder, in the pure and binary solvents, were weighed and then shaken at a constant temperature in the range 295−327 K in a temperature-controlled bath (±0.1 K). The loss of solvent, by evaporation, was avoided by condensing the vapor. The saturation concentration was reached after 4H (thermodynamic equilibrium), and then the solid phase was removed by filtration (Millipore millex hydrophobic membranes, 0.45 $\mu$m pore size). All filtration apparatus (syringes, filters, etc.) were previously heated in a drying oven. The drug did not significantly adsorb into the membrane. The supernatant solutions were diluted with THF and analyzed by HPLC (HPLC Merk, Lachrom, $CH_3CN/H_2O/CH_3COOH$). All experimental results were the average of at least two replicated experiments. The variation coefficient was within 4% among replicated samples.

**Metastable Zone Width Measurements.** The experiments were carried out in a 150-mL, round-bottomed Pyrex glass crystallizer (see Figure 4). The double-jacketed crystallizer was equipped with a lid, four baffles, a condenser, and a Pt-100 resistance thermometer. The precision of these thermometers is given to be 1/10 °C.

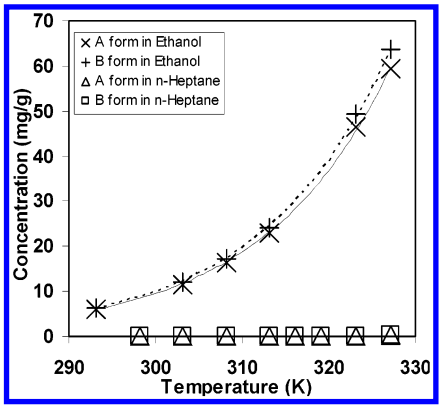


**Figure 5.** Solubilities of forms A and B of eflucimibe drug in pure ethanol and pure *n*-heptane.

The temperature control of the crystallizer was performed by a programmable thermostatic bath. The external (bath) and internal (solution) temperature profiles were recorded. For all the experiments, the stirring rate was taken equal to 250 rpm. The stirrer was driven by an electric motor with adjustable speed and analogue tachometer.

The metastable zone widths were determined as a function of the cooling rate in the range 5−20 °C/H for different initial concentrations of the solution. The ethanol/heptane/eflucimibe mixture was heated above 5 °C of the solubility temperature. To ensure complete dissolution, the temperature was kept constant for 15 min before each run. Then, the solution was cooled with a linear temperature profile (5, 10, 20 °C/H). Seeds ($m_{seed} \ll 1\%$) were added, if needed, when the system reached the solubility temperature. Nucleation was detected visually. No temperature rise was recorded for the nucleation onset. After crystallization, the solution was filtered and dried in a dry oven during 8H.

## Results and Discussion

**Phase Diagram.** Figure 5 shows the solubility profiles of the two forms A and B in pure ethanol and in *n*-heptane. The temperature range corresponds to the one used in the crystallization process. The temperature upper limit was fixed by the boiling point of ethanol (351 K).

The results show a relatively low solubility in ethanol and a very low solubility in *n*-heptane. In both cases, solubility increases with temperature, and the solubility profiles are smooth. The solubility differences between the two forms are very low (7% in pure ethanol).

In solvent mixtures, the solubility difference between the two forms A and B was less than 3% and at a constant solvent ratio, the solubility increased with temperature (see Figure 6 for form A). At a constant temperature, the solubility profiles show a maximum for a molar fraction of ethanol of $x_{EtOH} = 0.65$ in the ethanol/*n*-heptane mixture. This particular point corresponds to the azeotropic point of the mixture. In addition, the deviation from the additivity rule is more pronounced when increasing the temperature. This maximum solubility effect, or synergetic effect, was observed for a wide variety of systems,[6−8] and it can be explained by a decrease of the auto-association phenomenon of alcohols when increasing temperature, as well as by the stronger reactivity of the binary solvents.

The solubility data allowed choosing the ratio of solvent that was used in the process: the mixture that corresponds to the solubility maximum ($x_{EtOH} = 0.65$) was selected to enhance the crystallization efficiency.

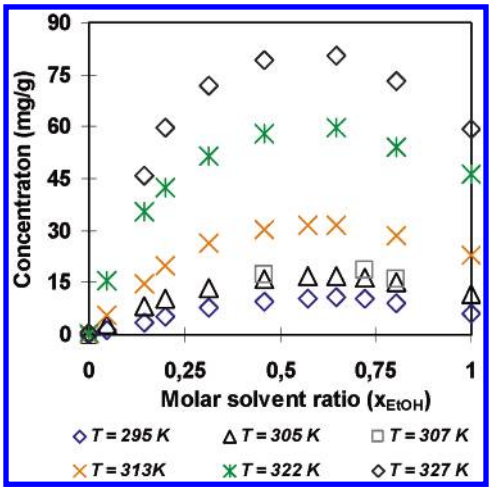


**Figure 6.** Experimental solubilities of eflucimibe (form A) obtained in different ethanol/*n*-heptane ratios [$x_{EtOH}$ = mol of ethanol/(mol of ethanol + mol of heptane)] and different temperatures.

**Metastable Zone Width.** The measurement of metastable zone width is a way of studying nucleation kinetics. Assuming that the A form is the stable polymorph, the solubility data of this form will be considered in these experiments and the solvent ratio used was $x_{EtOH} = 0.65$. Five initial concentrations of the solution corresponding to different initial temperatures along the solubility curve of form A, and three cooling rates have been tested. The experimental results obtained were analyzed in terms of metastable zone widths and polymorphism.

The metastable zone width was determined visually by detecting the appearance of the first(s) crystal(s). Of course, the visual determination of the nucleation (temperature) is quite subjective and the error was estimated to ±1.1 °C. The maximum allowable supersaturation may be expressed in terms of the maximum allowable undercooling. The oversimplification in the above analysis is that it assumes that at the moment when nuclei are first detected, the rate of supersaturation is equal to the rate of nucleation, but the true situation is rather more complex. In fact, in the experimental determination of the metastable limit, nuclei are not detected at the moment of their creation but at some later time when they have grown to a visible size (at, say, about 10 $\mu$m).

The results obtained without seeding are presented in Figure 7. Each result is the average of at least two replicated experiments. The maximum allowable undercoolings are more or less independent of the saturation temperature over the range 20−50 °C, but do depend on the rate of cooling. At low rates of cooling (5 °C/H), the values are about 30% lower compared with a cooling rate of 20 °C/H.

One set of experiments was performed with seeds, respectively, of form A and form B, for only one cooling rate (10 °C/H). A few seeds were introduced ($m < 0.1\%$) to induce secondary nucleation. The results are presented in Table 1.

Figure 8 shows the metastable zone widths with and without seeds for $V_c = 10$ °C/H.

The powder obtained during the metastable zone width measurements was characterized. As the crystal

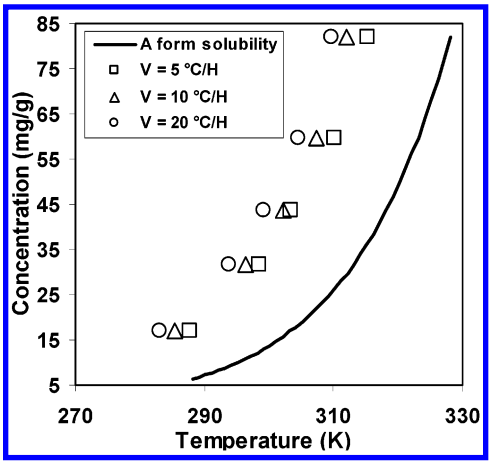


**Figure 7.** Experimental metastable zone widths of eflucimibe in ethanol/*n*-heptane mixture ($x_{EtOH} = 0.65$) obtained for different cooling rates without seeds.

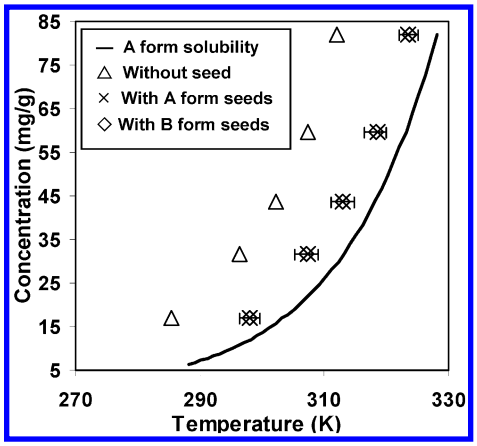


**Figure 8.** Comparison between experimental metastable zone widths of eflucimibe obtained with and without seeds in a ethanol/*n*-heptane mixture ($x_{EtOH} = 0.65$) at $V_c = 10$ (°C/H).

**Table 1. Comparison of the Experimental Metastable Zone Widths Obtained without Seeds and with Seeds of Form A or Form B Crystals of Eflucimibe in Ethanol/*n*-Heptane Mixtures ($x_{EtOH} = 0.65$) at $V_c = 10$ °C/H**

| initial conditions | | maximum allowable undercooling $\Delta T_{max}$ (K) | | |
|---|---|---|---|---|
| $C^*$ (mg/g) | $T_{sol}$ (K) | without seed | with A seeds | with B seeds |
| 16.86 | 304 | 16.49 (± 0.2) | 6.21 (± 0.9) | 6.15 (± 0.9) |
| 31.74 | 313 | 14.69 (± 0.3) | 5.85 (± 1.5) | 6.04 (± 1.4) |
| 43.53 | 318 | 14.65 (± 0.2) | 5.21 (± 0.9) | 5.22 (± 0.8) |
| 59.69 | 323 | 13.08 (± 0.3) | 4.65 (± 1.4) | 4.88 (± 1.5) |
| 81.89 | 328 | 12.93 (± 0.2) | 4.71 (± 0.9) | 4.51 (± 1.0) |

structures of A and B are unknown, quantitative phase analysis is impossible. Thus, the following procedure was adopted to estimate the phase fractions of A and B in the samples by DSC. The DSC scans obtained were compared to the one obtained for each pure polymorph. The results obtained by DSC on the crystallized powder without seeding are presented in Table 2.

In each case, a mixture of the two forms was obtained, and no rules or link between the polymorphs obtained and the initial temperature and cooling rate can be found. But, on one hand, at low initial concentration, the A form seems to be obtained, whereas, at higher concentrations ($C > 59.69$ mg/g) the B form was

**Table 2. Relative Polymorph Compositions of the Powder Obtained after Crystallization without Seeds in Ethanol/*n*-Heptane Mixture ($x_{EtOH} = 0.65$) at Different Cooling Rates**

| initial conditions $C^*$ (mg/g) | %A | | |
|---|---|---|---|
| | $V_c = 5$ °C/H (%) | $V_c = 10$ °C/H (%) | $V_c = 20$ °C/H (%) |
| 31.74 | 95 | 61 | 49 |
| 43.53 | 44 | 89 | 60 |
| 59.69 | 4 | 64 | 66 |
| 81.89 | 14 | 22 | 14 |

**Table 3. Relative Polymorph Composition of the Powder Obtained after Cooling Crystallization with Seeds in Ethanol/*n*-Heptane Mixture ($x_{EtOH} = 0.65$) at $V_c = 10$ (°C/H)**

| initial conditions $C^*$ (mg/g) | %A | | |
|---|---|---|---|
| | no seeds (%) | A seeds (%) | B seeds (%) |
| 31.74 | 61 | 100 | 92 |
| 43.53 | 89 | 100 | 93 |
| 59.69 | 64 | 59 | 100 |
| 81.89 | 22 | 38 | 100 |

obtained more easily. On the other hand, the cooling rate may play a role in the selectivity of the polymorphs.

The results obtained by DSC for the experiments performed at 10 °C/H with and without seeds are presented in Table 3.

From these results, it is clear that the seeds seem to control crystallization of eflucimibe. Indeed, when seeds of the B form were added, the B form was automatically obtained. However, when seeds of the A form were introduced, the A form was obtained for low initial concentration (or temperature), and at higher initial concentration, a mixture of the two forms was obtained (with a higher amount of A than in the nonseeded experiments).

**Kinetics Interpretations.** The results obtained for the metastable zone width measurements have been analyzed and interpreted in terms of nucleation kinetics. Two approaches have been used:[9] the first concerns the use of the Nylvt law to estimate roughly the rate of the primary nucleation (homogeneous or heterogeneous) and the maximum allowable undercooling. The second approach deals with the determination of the dominant nucleation mechanism in the crystallization process by the use of the Mersmann predominance diagram.[10]

**Determination of Nucleation Kinetics Law.** As the solution is free from foreign particles and the system is relatively slow, it appears reasonable to use the Nyvlt[11] law to describe the kinetics behavior of the eflucimibe/ethanol/*n*-heptane system. The nucleation rate, derived from the classical nucleation theory, is usually written as follows:

$$J = k_n \Delta c_{max}^n$$

Nyvlt has established that the nucleation rate may be expressed in terms of the rate at which supersaturation is created by cooling:

$$J = q\frac{dT}{dt}$$

$q$ is the mass of crystalline substance deposited per unit of mass of "free" solvent present when the solution is cooled by 1 °C. $q$ is a function of the concentration change and of the crystallizing species.

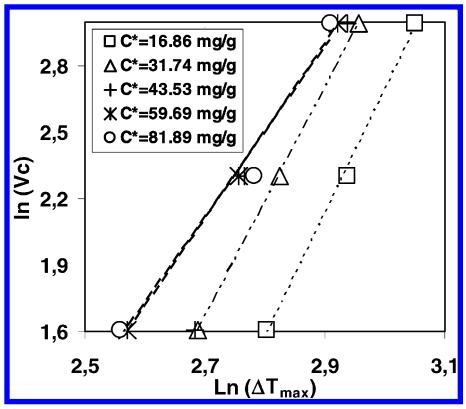


**Figure 9.** Variation of the cooling rate with the maximum allowable undercooling for eflucimibe in ethanol/*n*-heptane mixture (for $x_{EtOH} = 0.65$).

By identification of the two expressions, Nyvlt showed that the cooling rate ($dT/dt$) can be correlated to the maximum undercooling ($\Delta T_{max}$) by the relation:

$$\log\left(\frac{dT}{dt}\right) = (n-1)\log\left(\frac{dc^*}{dT}\right) + \log k_n + n \log \Delta T_{max}$$

which indicates that the dependence of the log($dT/dt$) on the log $\Delta T_{max}$ is linear (slope $n$). In those equations, $n$ is the apparent order of nucleation (but it is not a reliable indication of nucleation kinetics alone) and $k_n$ is the nucleation kinetics constant.

For eflucimibe, the experimental points given in Figure 7 were recalculated for drawing the maximum allowable undercooling $\Delta T_{max}$ versus the cooling rate $V_c = dT/dt$ for different initial concentrations of eflucimibe. The results are shown in Figure 9.

The lines of Figure 9 seem to show two different slopes ($n_1 = 5$, $n_2 = 4$) according to the initial concentration concerned. The change occurring around 43 mg/g could indicate that the nucleation mechanisms above and below this value are not exactly the same. But this must be considered by taking into account the experimental errors on the solubility and on the metastable zone widths measurements at high temperature (concentration). So the Nyvlt method gives an approximation of the primary nucleation apparent order: an average value around 4.5 can be taken and used in the following section.

**Identification of the Nucleation Mechanism.** Various mechanisms are proposed to correlate the nucleation process and the metastable zone width. Homogeneous primary nucleation ($B_{hom}$) occurs only if the supersaturated solution is free of any particle. On the contrary, heterogeneous primary nucleation ($B_{het}$) only occurs in the presence of foreign particles. Secondary nucleation requires the presence of crystals acting with the environment (walls, impeller), and nuclei originate from seeds or growing crystals ($B_{surf}$, $B_{att}$).[12,13] The rate of nucleation, $B$, is the sum of the contributions of different mechanisms that may occur in the crystallizer:

$$B = B_{hom} + B_{het} + B_{surf} + B_{att}$$

where $B_{hom}$, $B_{het}$, $B_{surf}$, and $B_{att}$ are the rate of homo-

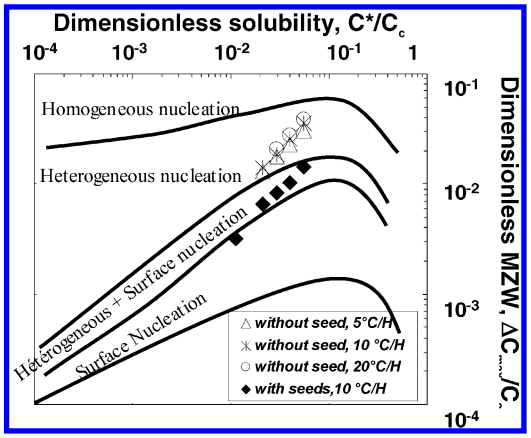


**Figure 10.** Estimation of the nucleation criterion according to Mersmann.

geneous nucleation (activated process), heterogeneous nucleation (activated process controlled by the quantity and quality of foreign particles), secondary surface nucleation (activated process controlled by surface nucleation and cluster formation), and the rate of attrition induced secondary nucleation (growth controlled). In general, one contribution is dominant in a given range of supersaturation.[14] For example, for highly soluble substances attrition is dominant, and for seeded crystallizer the surface nucleation mechanism is significant. In the case of a nonseeded crystallizer and poorly soluble substances, primary heterogeneous nucleation prevails.

Mersmann[10] has analyzed these different mechanisms in a diagram giving the dimensionless metastable zone width ($\Delta C_{max}/C_c$) versus the dimensionless solubility ($C^*/C_c$). Figure 10 reports this diagram with the different zones in which each mechanism prevails. The experimental points corresponding to eflucimibe metastable zone measurements, without and with seeding, were also reported in this diagram.

According to the results, the nonseeded metastable zone widths obtained are found to be governed by a primary heterogeneous nucleation mechanism, whatever the cooling rate and the initial concentration used. Whereas, when a seed is introduced, the system becomes activated by a secondary nucleation mechanism called "heterogeneous + surface nucleation". That is why, by adding "surface nucleation sites" with the desired polymorph, the crystallization is more efficiently controlled. So, to control polymorphism one could think to add a higher amount of A seeds to operate in the region of the diagram given in Figure 10, called "surface nucleation".

## Conclusion

In this study, the effect of the cooling rate, initial concentration, and "seeds" on polymorphism have been investigated to control the crystallization process of eflucimibe. The kinetic (metastable zone width) and thermodynamic (solubility) properties of the eflucimibe in a solvent mixture (ethanol/*n*-heptane) have been determined.

The two modifications A and B of eflucimibe are thermodynamically very close, and no interconversion is observed in the solid state. Solubility diagrams, and quench-cooling from the melt, which always leads to the B form, indicate that A is the long-term stable form.

The unseeded cooling crystallization yields, for most cases, to the metastable form B. In suspension, this form eventually transforms into the stable form A; however, the kinetics is very low (or the transformation is incomplete).

To make the crystallization process stable, a seeding procedure was chosen. For the unstable modification (B), seeding is always successful. On the contrary, for the stable modification (A form) seeding is unsuccessful for higher temperatures. So for scale-up purpose, a precise seeding policy will be built by increasing the amount of seeds introduced.

## Nomenclature

$B$, nucleation kinetics ($m^3/s$)
$C$, concentration (mg/g of solution)
$\Delta C_{max}$, maximum supersaturation (mg/g of solution or $kmol/m^3$)
$C^*$, solubility (mg/g of solution)
$C_C$, crystal molar density ($kmol/m^3$)
$J$, primary nucleation kinetics (kg/s)
$k_n$, nucleation kinetic constant, ($kg^{1-n}\ kg^{-(1-n)}\ s^{-1}$)
$n$, apparent order of nucleation
$T$, temperature (K)
$dT/dt$, cooling rate (°C/H)
$\Delta T_{max}$, maximum allowable undercooling (K)
$V_c$, cooling rate (°C/H)
$x_{EtOH}$, solubility (molar fraction)

*Subscript*

i, component i
Het, heterogeneous
Hom, homogeneous
Surf, surface nucleation
Att, nucleation induced by attrition

## References

(1) Bernstein, J. Conformational polymorphism. In *Organic Solid State Chemistry*; Desiraju, G. R., Ed.; Elsevier: Amsterdam, 1987; Chapter 13.
(2) Yu, L. Growth Rings in D-Sorbitol Spherulites: Connection to Concomitant Polymorphs and Growth Kinetics. *Cryst. Growth Des.* **2003**, *3*, 967−971.
(3) Yu, L.; Stephenson, G. A.; Mitchell, C. A.; Bunnell, C. A.; Snorek, S. V.; Bowyer, J. J.; Borchardt, T. B.; Stowell, J. G.; Byrn, S. R. Thermochemistry and Conformational Polymorphism of a Hexamorphic Crystal System. *J. Am. Chem. Soc.* **2000**, *122*, 585−591.
(4) Yu, L.; Reutzel-Edens, S. M.; Mitchell, C. A. Crystallization and Polymorphism of Conformationally Flexible Molecules: Problems, Patterns, and Strategies. *Org. Proc. Res. Dev.* **2000**, *4*, 396−402.
(5) Ribet, J. P.; Pena, R.; Chauvet, A.; Patoiseau, J. F.; Autin, J. M.; Segonds, R.; Basquin, M.; Autret, J. M. Polymorphisme cristallin de l'éflucimibe. *Ann. Pharm. Fr.* **2002**, *60*, 177−186.
(6) Domanska, U. Solubility of *n*-paraffin hydrocarbons in binary solvent mixtures. *Fluid Phase Equilib.* **1987**, *35*, 217−236.
(7) Domanska, U. Solubility of acetyl-substituted naphthols in binary solvent mixtures. *Fluid Phase Equilib.* **1990**, *55*, 125−145.
(8) Prausnitz, J. M.; Lichtenthaler, R. N.; Gomes de Azevedo, E. *Molecular Thermodynamics of Fluid-Phase Equilibria*, 3rd. ed.; Prentice Hall PTR: New York, 1998.
(9) Ulrich, J.; Strege, C. Some aspects of the importance of metastable zone width and nucleation in industrial crystallizers. *J. Cryst. Growth* **2002**, *237−239*, 2130−2135.
(10) Mersmann, A.; Bartosch, K. How to predict the metastable zone width. *J. Cryst. Growth* **1998**, *183*, 240−250.
(11) Nyvlt, J. Kinetics of nucleation in solutions. *J. Cryst. Growth* **1968**, *3−4*, 377−383.

(12) Mersmann, A. Crystallization and precipitation. *Chem. Eng. Proc.* **1999**, *38*, 345−353.
(13) Mersmann, A.; Braun, B.; Loffelmann, M. Prediction of crystallization coefficients of the population balance. *Chem. Eng. Sci.* **2002**, *57*, 4267−4275.
(14) Kim, K.-J.; Mersmann, A. Estimation of metastable zone width in different nucleation processes. *Chem. Eng. Sci.* **2001**, *56*, 2315−2324.

CG0341961